

Mutations in *RDH12* encoding a photoreceptor cell retinol dehydrogenase cause childhood-onset severe retinal dystrophy

Andreas R Janecke¹, Debra A Thompson^{2,3}, Gerd Utermann¹, Christian Becker⁴, Christian A Hübner⁵, Eduard Schmid⁶, Christina L McHenry², Anita R Nair², Franz Rüschenhoff⁴, John Heckenlively², Bernd Wissinger⁷, Peter Nürnberg^{4,8} & Andreas Gal⁵

We identified three consanguineous Austrian kindreds with 15 members affected by autosomal recessive childhood-onset severe retinal dystrophy, a genetically heterogeneous group of disorders characterized by degeneration of the photoreceptor cells¹. A whole-genome scan by microarray analysis of single-nucleotide polymorphisms (ref. 2) identified a founder haplotype and defined a critical interval of 1.53 cM on chromosome 14q23.3–q24.1 that contains the gene associated with this form of retinal dystrophy. *RDH12* maps in this region and encodes a retinol dehydrogenase proposed to function in the visual cycle³. A homozygous 677A→G transition (resulting in Y226C) in *RDH12* was present in all affected family members studied, as well as in two Austrian individuals with sporadic retinal dystrophy. We identified additional mutations in *RDH12* in 3 of 89 non-Austrian individuals with retinal dystrophy: a 5-nucleotide deletion (806delCCCTG) and the transition 565C→T (resulting in Q189X), each in the homozygous state, and 146C→T (resulting in T49M) and 184C→T (resulting in R62X) in compound heterozygosity. When expressed in COS-7 cells, Cys226 and Met49 variants had diminished and aberrant activity, respectively, in interconverting isomers of retinol and retinal. The severe visual impairment of individuals with mutations in *RDH12* is in marked contrast to the mild visual deficiency in individuals with fundus albipunctatus caused by mutations in *RDH5*, encoding another retinol dehydrogenase⁴. Our studies show that *RDH12* is associated with retinal dystrophy and encodes an enzyme with a unique, nonredundant role in the photoreceptor cells.

The three kindreds affected by autosomal recessive severe retinal dystrophy (Fig. 1) live in western Austria. Although genealogical studies could not link the families, relatedness seemed likely because

of geographic proximity and similar disease phenotype. Assuming a hypothetical founder more remote than nine generations, the region of homozygosity surrounding the disease locus should be ≤5 cM. We carried out a genome-wide search for homozygosity using a DNA microarray of >10,000 single-nucleotide polymorphisms (SNPs) on the GeneChip Human Mapping 10K Array. The chip could detect a region of homozygosity of ≤5 cM, and the analysis was accomplished in 3 days (ref. 2).

Affected individuals were homozygous, and obligate carriers heterozygous, with respect to ten SNPs (Table 1) in an interval of 2.86 Mb on chromosome 14q23.3–q24.1 (multipoint lod score of Z = 6.09 at θ = 0.00 for SNP rs52701). The boundaries were set between SNPs rs915056 and rs1954119 by two recombinants (data not shown). This interval overlapped with an interval containing a locus (*LCA3*) associated with a severe form of autosomal recessive retinal degeneration called Leber congenital amaurosis (LCA)⁵. We identified 29 genes in the critical interval in the annotated draft sequence of the human genome (Build 34). Of these, *RDH12* encodes a retinol dehydrogenase that belongs to the superfamily of short-chain alcohol dehydrogenases and reductases and is expressed predominantly in the neuroretina³. Enzymes of this group have a crucial role in the interconversion of vitamin A and 11-*cis* retinal, the light-absorbing chromophore of rhodopsin and cone opsins, in a process referred to as the visual cycle⁶. The gene is composed of seven exons and encodes a protein of 316 amino acids³.

We found a 677A→G transition in exon 6 of *RDH12* that changes Tyr226 to Cys226, which cosegregated with the retinal degeneration phenotype in all three families (Fig. 1). Tyrosine is conserved at this position in mouse, rat and bovine *RDH12* orthologs³. In addition to two noncoding SNPs, we identified another *RDH12* coding sequence change in affected individuals, a homozygous 482G→A transition in exon 5 (resulting in the amino acid substitution R161Q), which was

¹Institut für Medizinische Biologie und Humangenetik, Medizinische Universität Innsbruck, Innsbruck, Austria. ²Department of Ophthalmology and Visual Sciences and ³Department of Biological Chemistry, University of Michigan Medical School, Ann Arbor, Michigan USA. ⁴Gene Mapping Center, Max-Delbrück Center for Molecular Medicine, Berlin-Buch, Germany. ⁵Institut für Humangenetik, Universitätsklinikum Hamburg-Eppendorf, Butenfeld 42, D-22529 Hamburg, Germany. ⁶Klinik für Augenheilkunde, Medizinische Universität Innsbruck, Innsbruck, Austria. ⁷Klinik für Augenheilkunde, Universität Tübingen, Tübingen, Germany. ⁸Institut für Medizinische Genetik, Charité-Hochschulmedizin Berlin, Berlin, Germany. Correspondence should be addressed to G.U. (Gerd.Utermann@uibk.ac.at).

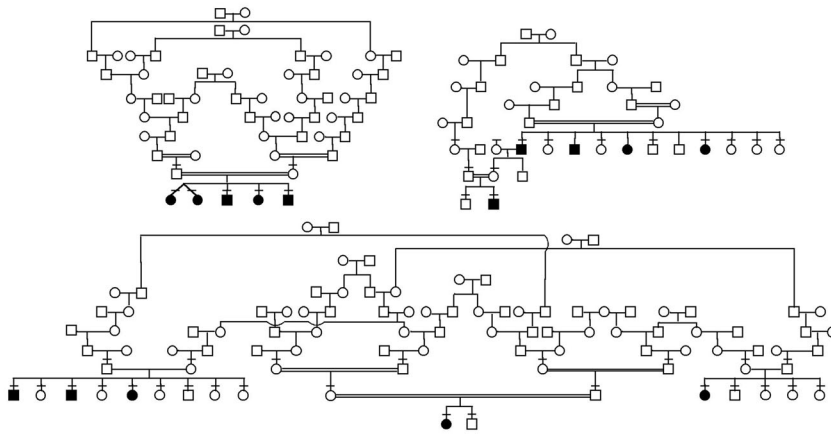


Figure 1 Pedigrees of three families in which retinitis pigmentosa and the *RDH12* mutation 677A→G segregated. Horizontal lines above pedigree symbols identify individuals who underwent ophthalmological investigation and were tested for cosegregation of the mutation with the disease phenotype.

also present in unaffected controls (27 of 154 alleles), indicating that it is a frequent polymorphism. In subsequent screening of 20 Austrian individuals with early-onset severe retinal degeneration who were not known to be related to the three families whom we originally studied, we identified two additional individuals who were homozygous with respect to the 677G allele. Both carry the same *RDH12* haplotype, consisting of three SNPs, that we observed in the affected individuals in the three families whom we originally studied (Table 1). Thus, 677A→G seems to be a founder mutation for retinal dystrophy in western Austria.

In 3 of 89 non-Austrian individuals with early-onset retinal degeneration, assumed to be unrelated to the three Austrian families whom we originally studied, we identified disease-associated mutations in *RDH12*. Individual 828, a German man diagnosed with LCA at the age of 4 years, carries an apparently homozygous 806delCCCTG deletion in exon 6. The resulting shift in reading frame is predicted to result in a premature stop codon at position 269. His parents carry the deletion in heterozygous state, as does his unaffected sister. Individual 839 is of Turkish origin and was diagnosed with LCA. His parents were cousins, and his older sister was also affected. He carries an apparently

homozygous 565C→T transition (resulting in Q189X). We genotyped his two unaffected siblings and found that one sister carries only wild-type *RDH12* sequence but the other sister is heterozygous with respect to 565C→T, as is his mother. Both 806delCCCTG and 565C→T probably result in protein truncation or nonsense-mediated mRNA decay, and in loss of *RDH12* activity. In individual 33, an American woman diagnosed with juvenile retinitis pigmentosa at the age of 5 years, we identified two heterozygous transitions in exon 2, 146C→T (resulting in T49M) and 184C→T (resulting in R62X). In the absence of parental DNA, we carried out restriction analysis of DNA from the affected individual to establish that the mutations were on different alleles (Fig. 2a). The locations of the disease-associated mutations in *RDH12* that we identified are shown in Figure 2c.

All individuals with mutations in *RDH12* suffered from retinal dystrophy affecting both rods and cones with onset of symptoms in early childhood (2–4 y) and progression to legal blindness in early adulthood (18–25 y). Fundus photography showed that individual 33 had widespread atrophy of the retinal pigment epithelium (RPE) and pronounced pigment deposits in the periphery (Fig. 2b), rarely seen in young individuals with retinal dystrophy with mutations in genes encoding other visual cycle components⁷. In general, individuals with mutations in *RDH12* had a relatively consistent and severe phenotype, with fundi showing pronounced attenuation of retinal arterioles and intraretinal bone spicule pigmentation. The electroretinogram (ERG) was extinguished at the time of the first investigation (as early as 5 and 6 years of age in two of the individuals).

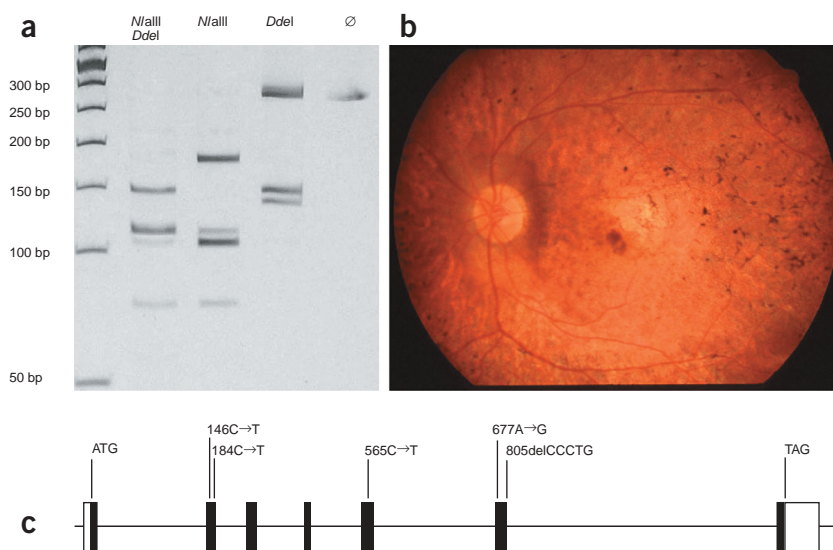
To analyze the effect of the *RDH12* missense variants identified in affected individuals on enzyme activity, we transfected COS-7 cells with *RDH12* cDNA in pcDNA3.1/His to express the full-length protein as a fusion containing an N-terminal epitope tag. We assayed *RDH12* activity in cell lysates in the presence of exogenous retinoids using normal phase high-performance liquid chromatography (HPLC). When NADPH was present as cofactor, lysates from cells expressing the wild-type protein catalyzed the conversion of all-*trans* retinal to all-*trans* retinol in a time- and concentration-dependent manner, resulting in 13 times more all-*trans* retinol than was generated by cells transfected with an empty vector ($P < 0.001$) in 30-min assays (Fig. 3a,b). The activity of the wild-type protein was also significantly different in the reverse reaction (conversion of all-*trans* retinol to all-*trans* retinal in the presence of NADP⁺), resulting in 1.88 times more all-*trans* retinal than was generated by cells transfected with an empty vector ($P < 0.02$; Fig. 3c). Lysates from cells expressing the Cys226 variant had no significant *RDH12* activity in the forward or reverse reactions, consistent with a loss of function of *RDH12*. The Met49 variant produced 22 times more all-*trans* retinol than the empty vector ($P < 0.001$), indicating that its activity was 1.90 times higher than that of the wild-type protein ($P < 0.02$). In contrast, the activity of the Met49 variant was 0.44 times lower than that of the wild-type protein in the reverse reaction ($P < 0.04$), generating 1.38 times more all-*trans* retinol than was generated by cells transfected with an empty vector ($P < 0.04$; Fig. 3c). We obtained correspondingly similar results for each of the variants in pcDNA3.1 constructs that expressed the proteins without the epitope tag, and in assays with 9-*cis* retinal or 11-*cis* retinal as substrate (data not shown).

Table 1 Haplotype carrying the 677A→G mutation of *RDH12*

Chromosome position (bp)	SNP	Allele
65368096	Rs728647	A
65473562	Rs1950284	G
66149667	Rs3742881 (<i>RDH11</i> intron 2)	T
66181403	<i>RDH12</i> intron 2	A
66181409	<i>RDH12</i> intron 2	A
66183772	<i>RDH12</i> exon 5 482G→A	A
66185967	<i>RDH12</i> exon 6 677A→G	G
66751027	Rs2877455	G
66761491	Rs911258	C
66763394	Rs2180770	T
66951606	Rs2331706	C
67057679	Rs2145157	C
67079527	Rs761951	A
67204999	Rs52701	A

Sequence variants in *RDH12* were identified by sequencing of DNA from affected individuals. The other SNPs were tiled on the GeneChip Human Mapping 10K Array.

Figure 2 Genotype and retinal phenotype of an individual with mutations 146C→T and 184C→T in *RDH12* and schematic of *RDH12* gene structure and disease-associated mutations. **(a)** Analysis of the allelic nature of the two *RDH12* mutations identified by restriction digestion analysis of amplicon 2 (301 bp). Mutation 146C→T results in an additional *Nla*III site, yielding mutation-specific fragments of 119 and 75 bp (from the wild-type 193-bp fragment) and an invariant 107-bp fragment (third lane of gel). Mutation 184C→T creates a new *Dde*I site that cuts the 301-bp wild-type fragment into fragments of 155 and 146 bp (fourth lane of gel). The results of *Dde*I and *Nla*III double digestion showing the fragments of 155, 119, 107, 75 and 39 bp indicate that the individual is compound heterozygous (second lane of gel). If the two sequence variants were on the same allele, fragments of 194, 119, 107, 39 and 36 bp would be expected. Uncut DNA is shown in the last lane of the gel. Fragments smaller than 50 bp were not resolved by the gel system used. **(b)** Fundus photograph of the individual's left eye taken at 5 years and 4 months of age, showing pronounced attenuation of retinal arterioles, pigment deposits in the periphery and widespread RPE atrophy with macular involvement. **(c)** Vertical lines indicate the sites of mutations on the *RDH12* gene structure. Exons are depicted as boxes and coding regions are filled in.



Western-blot analysis of RDH12 in total protein lysates from cells transfected with the wild-type fusion construct using an antibody against the epitope tag detected a main immunoreactive band at 35 kDa, and two minor bands at 41 and 43 kDa, that were not present in cells transfected with an empty vector (**Fig. 3d**). Treatment of the lysate with the deglycosidases PNGase F or Endo H (which cleave various forms of N-linked oligosaccharides) collapsed the three bands into one band, running at 35 kDa (data not shown). We suggest that this latter band corresponds to the unglycosylated protein and the two other bands to differentially glycosylated forms. Cells transfected with the Met49 variant showed a protein pattern similar to that of the wild-type, but with less unglycosylated protein present. In contrast, the expression of all three forms of the protein was decreased in cells transfected with the Cys226 variant (**Fig. 3d**). The results of immunohistochemical analysis of transfected COS-7 cells were consistent with a similar subcellular localization for each of the variants (**Fig. 3e**). Taken together, the results of our analyses suggest that Y226C and T49M affect RDH12 protein expression and activity, although the mechanism involved seems to be different in each case.

Our data identify RDH12 as a key and nonredundant enzyme of the visual cycle by showing that mutations of RDH12 are associated with childhood-onset severe retinal degeneration. Disease-associated mutations were previously identified in several genes expressed in the RPE that encode proteins of the visual cycle, including *RPE65*, *RLBP1*, *RDH5*, *RGR* and *LRAT* (reviewed in ref. 7). The pathomechanism of mutations in *RPE65* is thought to involve spontaneous, light-independent opsin activity due to loss of the 11-*cis* retinal chromophore⁸. As mutations in *RDH12* are also predicted to decrease 11-*cis* retinal synthesis, constitutive opsin activity may also contribute to disease development in this way. Alternatively, or in addition, accumulation of all-*trans* retinal in the photoreceptors may be detrimental.

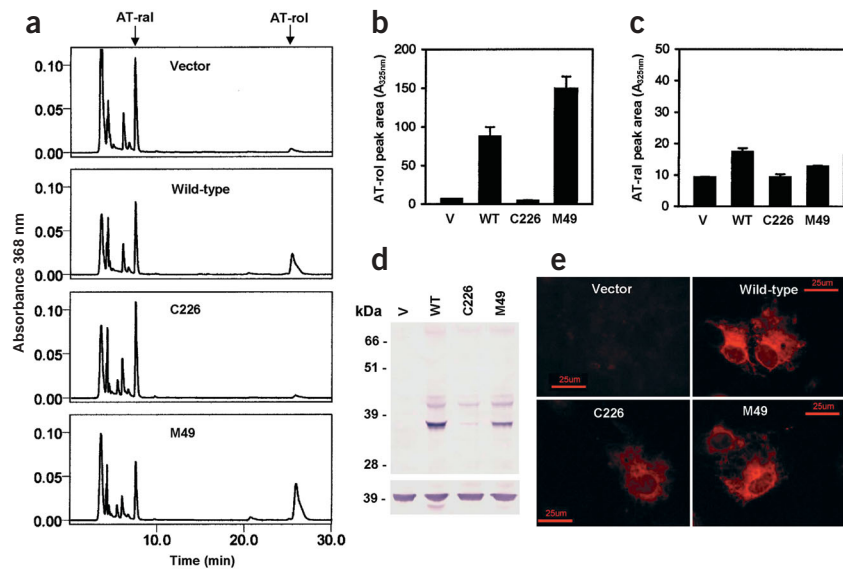
Recent studies described RDH12 as a new dehydrogenase/reductase present in the photoreceptor cells with dual specificity for *cis*- and all-*trans* retinoid substrates³. Previous studies identified two other retinoid dehydrogenases expressed in photoreceptors, retSDR1 (ref. 9) and prRDH10, with the ability to catalyze the reduction of all-*trans* retinal to all-*trans* retinol. The existence of such redundancy might predict that loss-of-function mutations in any one gene would produce only mild functional deficits or no abnormalities at all. In fact, this is the case for *RDH5*, encoding an 11-*cis* retinoid dehydrogenase of the RPE, mutations of which result in a nonprogressive night blindness without retinal dystrophy (fundus albipunctatus)⁴. The severe phenotype associated with mutations in *RDH12* suggests that RDH12 has a unique role in the visual cycle and offers new insight into the importance of this class of enzymes. Understanding this role will require determining whether the primary function of RDH12 is in the rods or cones, or both. A number of therapeutic approaches to treat genetic defects affecting the visual cycle in the RPE are currently under development. Our finding of mutations in *RDH12* offers new incentive for extending these efforts to the treatment of defects in the photoreceptors themselves.

METHODS

Affected individuals and phenotypes. Informed consent was obtained from all participants, and protocols were approved by the institutional review boards of the Universitaet Innsbruck, University of Michigan, Universitaetsklinikum Hamburg-Eppendorf and Universitaet Tübingen. We purified DNA from venous blood or buccal smears. Affected and unaffected family members included in the DNA study underwent ophthalmoscopy. In addition, ten homozygous individuals and four heterozygous carriers with respect to the 677A→G mutation underwent electroretinography.

In adults with the 677A→G mutation on both *RDH12* alleles, fundi had massive intraretinal bone spicule pigmentation in the mid periphery, optic discs had a waxy appearance, and there was a pronounced attenuation of retinal

Figure 3 Expression analysis and retinol dehydrogenase activity in transfected COS-7 cells. Cells were transfected with *RDH12* constructs in pcDNA3.1/HIS vector that express the protein as a fusion with the Xpress epitope. (a) HPLC analysis of all-*trans* retinol formation in cell lysates supplemented with NADPH and all-*trans* retinal. Representative traces are shown. The positions in the chromatogram where all-*trans* retinal (substrate) and all-*trans* retinol (product) elute are indicated at the top. The peaks in the chromatogram preceding all-*trans* retinal represent other retinal isomers and retinyl esters. (b) Data (mean \pm s.d. of three replicates) from HPLC assays of all-*trans* retinol formation as in a, quantified by integrating the area under the 325-nm peak (μ Vs/10,000). (c) Data (mean \pm s.d. of three replicates) from HPLC assays of all-*trans* retinol formation in cell lysates supplemented with NADPH and all-*trans* retinol, quantified by integrating the area under the 368-nm peak (μ Vs/10,000). (d) Western-blot analysis of cell lysates probed with antiserum against the Xpress epitope (upper) or with GAPDH antibody (lower). (e) Immunohistochemical analysis of transfected cells probed with antiserum against the Xpress epitope. V, empty vector; WT, wild-type; AT-ral, all-*trans* retinal; AT-rol, all-*trans* retinol. The data shown are representative of three independent transfection experiments.



arterioles. The ERG was extinguished at the time of the first investigation, notably at 6 years of age in one individual.

At age 19, individual 828 (homozygous with respect to 806delCCCTG) had visual acuity of light perception in the right eye and 0.05 in the left eye. Both scotopic and photopic ERGs were extinguished, and the fundi showed heavy hyperpigmentation with bone spicule-like pattern. A secondary vasoproliferative process with Coats-like structures was present in the right eye.

Individual 839 (homozygous with respect to 565C \rightarrow T) was diagnosed with LCA at the age of 2 years. He has one brother and four sisters; one sister also has LCA. At age 23, the individual had visual acuity of 0.05 in each eye, with visual fields showing concentric constriction to $\sim 10^\circ$ for large and bright stimuli (V4e). In the left eye, an eccentric small island of $\sim 10^\circ$ in diameter remained. There was a horizontal pendular nystagmus and many errors in the panel D15 color vision test. Only rudimentary ERG responses were present, pointing to advanced tapetoretinal degeneration. Funduscopy showed an atrophic optic disc with extremely narrow retinal vessels and large areas of choroidal atrophy with pigment clumps. A posterior subcapsular cataract was present. Ten years later, the individual had visual acuities of light perception in the right eye and hand movement in the left eye, there was no visual field for the right eye for the V4e isopter, and a small temporal field at $\sim 30^\circ$ for the left eye. Scotopic Ganzfeld-ERG, including 10-Hz flicker, did not show any considerable rod responses. Photopic ERG responses were also absent.

Individual 33 (146C \rightarrow T and 184C \rightarrow T) is the second of three children of nonconsanguineous parents. She was found to be night-blind at 2 years of age, she failed her vision screening test at age 4, and she was diagnosed with juvenile retinitis pigmentosa at age 5. At that time, she had micronystagmus, visual acuity of 0.5 in the right eye and 0.67 in the left eye and diffuse atrophy of the RPE throughout the equator area. The fundus reflex had a beaten metal appearance, photopic ERG was unrecordable, and scotopic ERG was barely recordable. The disease progressed continuously, with best corrected vision of 0.067 in the right eye and 0.01 in the left eye at her current age of 22 years, moderately heavy bone spicule pigmentation, diffuse RPE atrophy, a central scotoma and multiple blind spots scattered throughout each eye. None of her immediate family members have any symptoms of retinal disease.

Genotyping and linkage analysis. We genotyped DNA samples from ten affected individuals and nine mutation carriers from the three Austrian kindreds

by whole-genome sampling analysis² using the Affymetrix GeneChip Human Mapping 10K Array version Xba131. The median physical distance between SNPs and their average heterozygosity were 105 kb and 0.37, respectively, predicting an average spacing of informative 'markers' of > 1 Mb. Genotypes for 11,555 SNPs (10,894 autosomal, 301 X-linked and 360 lacking a position in the draft sequence of human genome, build 34) were called by the GeneChip DNA Analysis Software (GDAS v2.0, Affymetrix). We verified sample genders by counting heterozygous SNPs on the X chromosome. We detected relationship errors among samples from families using the program Graphical Relationship Representation (GRR)¹¹. We used the program PedCheck to detect mendelian errors¹² and removed data for SNPs with such errors, as well as uninformative SNPs, from the data set. We identified nonmendelian errors using the program Merlin¹³ and deleted unlikely genotypes for related samples. We carried out nonparametric linkage analysis using all genotypes from a chromosome simultaneously, using the program Merlin. We carried out parametric linkage analysis with a modified version of the program Genehunter 2.1 (refs. 14,15). The analysis was done stepwise using a subset of markers in the way of a nonoverlapping moving window that covered 50–300 SNPs. We used the programs Merlin and Genehunter to reconstruct haplotypes.

Mutation screening. We amplified all seven exons of *RDH12* using standard PCR conditions and oligonucleotide primers corresponding to intronic sequences. We carried out mutation screening using denaturing HPLC on a WAVE DNA Fragment Analysis System (Transgenomic) or single-strand conformation analysis with 8% glycerol. We sequenced fragments with an abnormal retention or electrophoresis pattern on an ABI 310 DNA sequencer using BigDye terminator mix (Applied Biosystems). Primer sequences and screening conditions are available on request. We found none of the mutations most likely to be associated with disease in 50 unaffected individuals. We also found no disease-associated mutations in *RDH11*, a gene encoding another retinol dehydrogenase of the visual cycle, which is also present in the critical genetic interval. Our analysis identified a number of rare *RDH12* sequence variants not likely to be pathogenic, as they were present in both affected and unaffected individuals (–152A \rightarrow G, IVS2+60G \rightarrow A, IVS2+54A \rightarrow T, 195A \rightarrow C and IVS7+54G \rightarrow C).

In vitro mutagenesis, expression and enzyme assay. We amplified *RDH12* cDNA (482G allele), including 10 bp of 5' and 32 bp of 3' untranslated

sequences, from human total retinal RNA by RT-PCR, cloned it into pGEM-T (Promega) and subcloned it into pcDNA3.1/HIS, expressing the recombinant protein as a fusion with Xpress epitope (Invitrogen). We introduced the mutations found in affected individuals using the QuikChange Kit (Stratagene). We verified the constructs by DNA sequencing.

We transiently transfected COS-7 cells with mutant or wild-type *RDH12* constructs, or with empty vector, using FuGene6 (1 µg of DNA per 3 µl of reagent) according to the manufacturer's instructions (Roche) and collected them 44 h after transfection. We included an expression construct for β-galactosidase (pCMV-βgal; 5% of total DNA) to control for transfection efficiency (assayed using *o*-nitrophenyl-*D*-galactopyranoside staining). β-galactosidase assays of lysates from cotransfected cells showed that all constructs were transfected with equal efficiency.

For western-blot analysis of fusion protein expression, we dissociated cells in SDS sample buffer, separated them by electrophoresis on NuPage Novex Bis-Tris acrylamide gels (Invitrogen) with SeeBlue Plus2 standards (Invitrogen), transferred them to nitrocellulose and incubated them with Xpress antibody (Invitrogen) and then with alkaline phosphatase-conjugated antibody to mouse IgG (Molecular Probes). We verified equivalent protein loading by Coomassie blue staining and analysis of glyceraldehyde-3-phosphate dehydrogenase (GAPDH) immunoreactivity (Ambion). For analysis of *RDH12* glycosylation status, we treated denatured cell lysates with either Endo H or PNGase F endoglycosidases according to the manufacturer's instructions (New England Biolabs) before western transfer.

To quantify *RDH12* transcripts, we isolated total RNA from transfected cells using RNeasy (Qiagen) and synthesized first-strand cDNAs using MMLV-RT (Amersham). We amplified PCR products (327 bp) using forward and reverse primers located in exon 5 and exon 6, respectively. We monitored the reaction progress with Sybr Green (Molecular Probes) using a Corbett Rotorgene Thermocycler RG 3000 and normalized data against amplification reactions for human hypoxanthine phosphoribosyltransferase (236 bp product). The constructs had thresholds that differed from one another by one cycle number or less.

For *in vitro* analysis of *RDH12* activity, we collected cells in 25 mM Tris acetate (pH 7), 0.25 M sucrose and 1 mM dithiothreitol and disrupted them by sonication. We assayed enzyme activity in the presence of 200 µM of NADPH or NADP⁺ in 200-µl reactions containing 10 mM HEPES buffer (pH 7), 1 mM dithiothreitol, 0.5 mg ml⁻¹ of bovine serum albumin, 6 µg of cellular protein and 100 µM all-*trans* retinol, all-*trans* retinal, 9-*cis* retinal or 11-*cis* retinal (calculated using extinction coefficients in ref. 16), according to published methods³. After a 30-min incubation, reactions were stopped by addition of 300 µl of methanol, and retinoids were extracted with *n*-hexane (300 µl). The concentration of exogenous retinoids used in the assay was not rate limiting, and product formation was linear during the reaction period, as well as with respect to amount of added protein (data not shown). We identified retinoids in the extracts and quantified them by HPLC analysis using a Waters Alliance Separation Module and Photodiode Array Detector with a Supelcosil LC-31 column (25 cm × 4.6 mm, 3 µm) developed with 5% 1,4-dioxane in hexane. We identified peaks by comparison with retention times of standard compounds and evaluation of wavelength maxima. Quantitative analysis was done by comparing peak areas at 325 nm for retinol isomers and 368 nm for retinal isomers. We analyzed data using ANOVA ($\alpha = 0.05$; Excel software) and determined statistical differences at $P < 0.05$.

GenBank accession numbers. *RDH11*, NM_016026; 482G allele of *RDH12*, XM_085058; 482A allele of *RDH12*, NM_152443; chromosome 14 contig, NT_026437.1.

ACKNOWLEDGMENTS

We thank G. Huber and J. Oversier for technical assistance and W. Göttinger for discussions. This work was supported by grants from Tiroler Medizinischer Forschungsfond, Fond zur Förderung der Wissenschaftlichen Forschung in Österreich, the German Federal Ministry of Science and Education through the National Genome Research Network, EVI-GENORET, the Deutsche Forschungsgemeinschaft, the Forschungsförderungs fonds FM, UKE, the National Institutes of Health, the Foundation Fighting Blindness and Research to Prevent Blindness.

COMPETING INTERESTS STATEMENT

The authors declare that they have no competing financial interests.

Received 8 March; accepted 8 June 2004

Published online at <http://www.nature.com/naturegenetics/>

- Rivolta, C., Sharon, D., DeAngelis, M.M. & Dryja, T.P. Retinitis pigmentosa and allied diseases: numerous diseases, genes, and inheritance patterns. *Hum. Mol. Genet.* **11**, 1219–1227 (2002).
- Kennedy, G.C. *et al.* Large-scale genotyping of complex DNA. *Nat. Biotechnol.* **21**, 1233–1237 (2003).
- Haeseleer, F. *et al.* Dual-substrate specificity short chain retinol dehydrogenases from the vertebrate retina. *J. Biol. Chem.* **277**, 45537–45546 (2002).
- Yamamoto, H. *et al.* Mutations in the gene encoding 11-*cis* retinol dehydrogenase cause delayed dark adaptation and fundus albipunctatus. *Nat. Genet.* **22**, 188–191 (1999).
- Stockton, D.W. *et al.* A novel locus for Leber congenital amaurosis on chromosome 14q24. *Hum. Genet.* **103**, 328–333 (1998).
- McBee, J.K., Palczewski, K., Baehr, W. & Pepperberg, D.R. Confronting complexity: the interlink of phototransduction and retinoid metabolism in the vertebrate retina. *Prog. Retin. Eye Res.* **20**, 469–529 (2001).
- Thompson, D.A. & Gal, A. Vitamin A metabolism in the retinal pigment epithelium: genes, mutations, and diseases. *Prog. Retin. Eye Res.* **22**, 683–703 (2003).
- Woodruff, M.L. *et al.* Spontaneous activity of opsin apoprotein is a cause of Leber congenital amaurosis. *Nat. Genet.* **35**, 158–164 (2003).
- Haeseleer, F., Huang, J., Lebioda, L., Saari, J.C. & Palczewski, K. Molecular characterization of a novel short-chain dehydrogenase/reductase that reduces all-*trans*-retinal. *J. Biol. Chem.* **273**, 21790–21799 (1998).
- Rattner, A., Smallwood, P.M. & Nathans, J. Identification and characterization of all-*trans*-retinol dehydrogenase from photoreceptor outer segments, the visual cycle enzyme that reduces all-*trans*-retinal to all-*trans*-retinol. *J. Biol. Chem.* **275**, 11034–11043 (2000).
- Abecasis, G.R., Cherny, S.S., Cookson, W.O. & Cardon, L.R. GRR: graphical representation of relationship errors. *Bioinformatics* **17**, 742–743 (2001).
- O'Connell, J.R. & Weeks, D.E. PedCheck: a program for identification of genotype incompatibilities in linkage analysis. *Am. J. Hum. Genet.* **63**, 259–266 (1998).
- Abecasis, G.R., Cherny, S.S., Cookson, W.O. & Cardon, L.R. Merlin - rapid analysis of dense genetic maps using sparse gene flow trees. *Nat. Genet.* **30**, 97–101 (2002).
- Kruglyak, L., Daly, M.J., Reeve-Daly, M.P. & Lander, E.S. Parametric and nonparametric linkage analysis: a unified multipoint approach. *Am. J. Hum. Genet.* **58**, 1347–1363 (1996).
- Strauch, K. *et al.* Parametric and nonparametric multipoint linkage analysis with imprinting and two-locus-trait models: application to mite sensitization. *Am. J. Hum. Genet.* **66**, 1945–1957 (2000).
- Garwin, G.G. & Saari, J.C. High-performance liquid chromatography analysis of visual cycle retinoids. *Methods Enzymol.* **316**, 313–324 (2000).

Corrigendum: TGF β signaling in health and disease

R J Akhurst

Nat. Genet. 36, 790 (2004).

On page 791, in the second column, the second full sentence should begin, “Camurati-Engelmann syndrome, a bone overgrowth defect due to TGF β 1 missense mutations...”

Corrigendum: A functional variant of SUMO4, a new I κ B α modifier, is associated with type 1 diabetes

D Guo, M Li, Y Zhang, P Yang, S Eckenrode, D Hopkins, W Zheng, S Purohit, R H Podolsky, A Muir, J Wang, Z Dong, T Brusko, M Atkinson, P Pozzilli, A Zeidler, L J Raffel, C O Jacob, Y Park, M Serrano-Rios, M T Martinez Larrad, Z Zhang, H-J Garchon, J-F Bach, J I Rotter, J-X She & C-Y Wang

Nat. Genet. 36, 837–841 (2004).

On page 837, in the right column, the first full sentence should begin, “The G variant of this SNP had a higher frequency in affected individuals from the US (62.7%) than in matched controls (52.4%; $P = 0.0008$)...”

In Figure 2, the arrow indicating the direction of transcription of *SUMO4* should be pointing to the right.

The version of Supplementary Table 1 that initially appeared online was incorrect and has been replaced with the correct version.

Corrigendum: Mutations in *RDH12* encoding a photoreceptor cell retinol dehydrogenase cause severe childhood-onset retinal dystrophy

A R Janecke, D A Thompson, G Utermann, C Becker, C A Hübner, E Schmid, C L McHenry, A R Nair, F Rüschemdorf, J Heckenlively, B Wissinger, P Nürnberg & A Gal

Nat. Genet. 36, 850–854 (2004).

In Figure 2c, “805delCCCTG” should read “806delCCCTG”. In Figure 3, the y axis in panel a should read “Absorbance 325 nm” and the y axis in panel c should read “AT-ral peak area ($A_{368\text{nm}}$)”.